



# **RUBBLE ICE TRANSPORT ON ARCTIC OFFSHORE STRUCTURES (RITAS), PART I: SCALE-MODEL INVESTIGATIONS OF LEVEL ICE ACTION MECHANISMS**

Nicolas Serré <sup>1</sup>, Knut Høyland <sup>2</sup>, Trine Lundamo <sup>1</sup>, Basile Bonnemaire <sup>1</sup>, Karl-Ulrich Evers <sup>3</sup>,  
Arne Gürtner <sup>4</sup>

<sup>1</sup> Multiconsult, Tromsø, NORWAY

<sup>2</sup> Sustainable Arctic Marine and Coastal Technology (SAMCoT), Centre for Research-based  
Innovation (CRI), Norwegian University of Science and Technology, Trondheim, NORWAY

<sup>3</sup> HSVA, Hamburg, GERMANY

<sup>4</sup> Statoil, Trondheim, NORWAY

## **ABSTRACT**

A model scale experiment on the interaction between level ice and an arctic offshore structure with a downward bending hull was conducted in April 2012 in the large ice tank of HSVA. The experiment investigated the different mechanical processes contributing to the ice action. The present paper is completed by a companion paper “*Rubble Ice Transport on Arctic Offshore Structures (RITAS), part II: 2D scale-model study of the level ice action*”. Detailed investigations on special aspects of the level ice action mechanisms are presented in “*Rubble Ice Transport on Arctic Offshore Structures (RITAS), part III: Analysis of scale-model rubble ice stability*” and “*Rubble Ice Transport on Arctic Offshore Structures (RITAS), part IV: Tactile sensor measurement of the level ice load on inclined plate*”.

The structure is inclined at the waterline and promotes a downward bending failure of the level ice. Several parameters are varied: structure width, ice incidence, ice thickness, ice elastic modulus, ice density, ice velocity. The structure front is vertically divided in three sections allowing independent measurement of the load at the waterline and the load from the accumulated ice rubble. The experimental results show that the level ice load is affected by the ice rubble accumulation up to a certain ice rubble amount. A lower ice density increases the ice load due to the increased ice rubble buoyancy. For the selected aspect ratios, a doubling of the structure width increased the rubble load but not the waterline load.

## INTRODUCTION

The level ice action on offshore structures can generally be reduced by designing the structure geometry such that a bending failure of the level ice is promoted. The downward breaking of ice on large structure produces subsurface rubble ice accumulating under the incoming level ice and travelling along the structure's hull. The accumulated rubble ice has been acknowledged as one important component of the ice action in several ice interaction scenarios, for instance:

- Ice ridge interaction
- Level ice action on sloped structures

For ice ridge impact, Serré and Liferov (2010) have shown that the rubble accumulating under an ice ridge during the interaction with a vertical structure caused a surcharge effect which increased the unconsolidated keel load by 50% in the case they have studied.

Level ice action on sloped structure can be computed according to the guidelines given in ISO19906 (2010), based on Croasdale (1980) and Croasdale et al. (1994). The horizontal ice action component  $F_H$  is determined by Eq. ( 1)

$$F_H = \frac{H_B + H_P + H_R + H_L + H_T}{1 - \frac{H_B}{\sigma_f l_c h}} \quad (1)$$

where  $H_B$  is the ice breaking load,  $H_P$  is the load component required to push the ice sheet through the ice rubble,  $H_R$  is the load to push the ice blocks up the slope through the ice rubble,  $H_L$  is the load required to lift the ice rubble on top of the advancing ice sheet prior to breaking it, and  $H_T$  is the load to turn the ice block at the top of the slope.

The rubble accumulation onto the ice is affecting the terms  $H_P$ ,  $H_R$ , and  $H_L$ . Its influence on the horizontal ice action can be demonstrated through a simple exercise:

Given the parameters of Table 1, the horizontal ice action on a downward bending plane is computed from ISO 19906 (2010) as:

- 1.6 MN with no ice rubble accumulation
- 3.2 MN with a 3 m thick ice rubble accumulation.

Table 1. Arbitrary ice and structures parameters for verification of rubble effect

Ice	Flexural strength	Young modulus	Ice-structure friction	Density	Friction angle	Cohesi on	Rubble porosity	Ice-ice friction	Ice thickness
	0.22 MPa	4 GPa	0.15	920 kg/m <sup>3</sup>	40°	15 kPa	0.3	0.1	1 m
Structure	Width			Slope angle					
	60 m			45°					

The influence from the ice rubble on the ice action requires a correct estimation of the subsurface rubble transport and accumulation in order to obtain:

- An accurate computation of the design level ice action on a sloped structure
- A correct calibration of ice load mathematical models based on post simulation of model ice basin tests

Frederking and Timco (1985) have performed model tests of the level ice interaction with an upward inclined plate and derived analytical expressions for the ice loads but did not consider specifically the ice rubble. Underwater monitoring of the rubble motion during the interaction between broken ice and a plate which could be inclined upward or downward are reported in Timco (1991) together with measurements of the vertical load distribution. Paavilainen et al. (2011; 2013) investigated numerically the level ice failure and rubble effect on an upward inclined plate.

The present experiment is a parametric study of the interaction between level ice and a downward sloping structure. The structure is vertical below the downward slope at the waterline, and the experiment focuses on the subsurface rubble and the different mechanical processes contributing to the ice action. The experiment consisted of:

- Ice interaction with a downward bending structure (this paper)
- Ice interaction with a section of the structure encased in a transparent box (buoyancy box), for:
  - 2D study of the ice breaking process (Part II, Serré et al., 2013, and part IV, Lu et al., 2013):
  - Mechanical characterization of the subsurface rubble (Part II, Serré et al., 2013, and part III Kulyakhtin et al., 2013)

The set-up and main results of the structure interaction tests are described in the present paper.

## **EXPERIMENTAL SET UP**

5 ice sheets interacted with the structure (5 test series numbered 1000, 2000, 3000, 4000, and 5000). Series 1000 and 2000 had similar ice properties, while one ice property was changed in the three remaining test series. The experimental set up and tests matrix are presented in this section.

### ***Ice tank***

The experiments are performed in the large ice tank at HSVA. The tank is 78 m long, 10 m wide and 2.5 m deep. A 12 m long and 5 m deep water section is available at the end of the tank. The basin is equipped with a motor driven towing carriage that weighs 50 tons and provides speeds from 1 mm/s to 3000 mm/s and a maximum towing force of 50 kN.

### ***Models***

The structure had an inclined surface at the waterline, causing ice bending failure and creation of subsurface rubble ice. The lower part of the structure is vertical (Figure 1), causing accumulation of the subsurface rubble ice. A bottom element was inserted underneath the structure into the HSVA tank to reduce the water depth to 1.34 m.

The structure was divided into two identical sub-structures (port and starboard, mirror symmetry) which could be jointed or separated. The distance between the two parts in the separated mode was 1.08 m. A picture and sketches are given in Figure 1. Relevant structure characteristics for the interaction tests were:

- 1.2 m foot width (each sub-structure), 1.35 m waterline width, 45° slope angle, ice spoiler at 0.75 cm water depth
- Variable incidence in the horizontal plane (0°, 15°, 30°, and 45°), rotation axis behind the starboard sub-structure (disc in Figure 1c)

- Distance to the basin walls (at the waterline):
  - Joint mode, 3.88 m on the portside and 3.33 m on starboard
  - Separated mode, 2.8 m on the portside and 3.33 m on starboard.

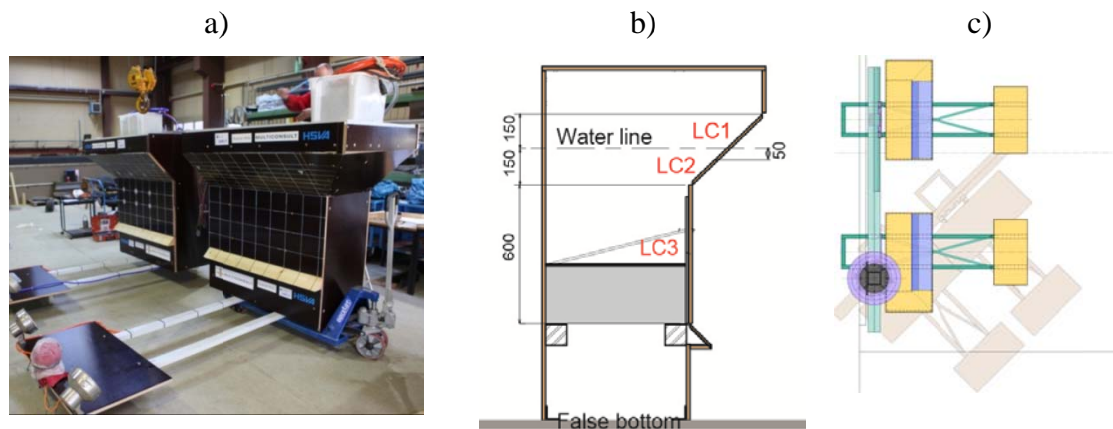


Figure 1. In a), picture of the two sub-structures; in b) cross section sketch; in c) sky view, variable incidence, here 0° separated and 45° joint (shadow).

### ***Load monitoring***

Each sub-structure was composed of three independent load measuring areas LC1, LC2, and LC3 (see Figure 1 and Table 2). LC1 extended 5 cm below the waterline and measured the loads from the ice interaction at the waterline. LC3 covered the vertical part of the structure over the spoiler and measured loads from the sub-surface rubble interacting with the panel.

Table 2. Load cell set-up.

<b>Load area</b>	<b>Position</b>	<b>Load cell set-up</b>	<b>Remarks</b>
LC1	Inclined panel, from 5 cm under the waterline and up (20 cm vertical distance)	2 tri-axial	1 damaged load cell in: - Portside part, series 1000 - Starboard part, series 2000
LC2	Inclined panel, from 5 cm under the waterline until vertical foot (10 cm vertical distance)	2 tri-axial	Contact between panel LC2 and LC3 on the portside part, series 1000
LC3	Vertical foot, from 15 cm under the waterline until the ice spoiler (60 cm vertical distance)	1 6-component	

During test series one load cell of LC1 panel on portside (test series 1000) and one load cell of LC1 panel on starboard (test series 2000) were damaged. In the present paper, LC1 loads from test series 1000 and 2000 are thus not presented.

### ***Video monitoring***

The transport of the subsurface rubble was monitored with 3 underwater video cameras: one in front of each sub-structure and one on the starboard of the structure. A grid was painted on the structure for easier determination of the rubble depth.

### *Ice characteristics*

For each test series, the structure interacted with model level ice and with a model ice rubble field. The ice properties were measured according to the methods described in Schwarz et al. (1981) and Evers and Jochman (1993), and are given in Table 3.

Table 3. Ice properties for the different ice sheets

Parameter	Unit	Test 1000	Test 2000 (High velocity)	Test 3000 (Low density)	Test 4000 (High thickness and E- module)	Test 5000 (Low E- module)
Ice thickness	cm	4.3	4.3	4.7	6.1	4.1
Flexural strength	kPa	53	58.2	54.6	45.7	47.1
Elastic modulus	MPa	61	53	88	103	31
Ice-structure friction				0.018		
Ice density	kg/m <sup>3</sup>	906	902	806	928	894
Ice salinity	‰	Approximately 3.5				
Water density	kg/m <sup>3</sup>	1006				
Water salinity	‰	6.9				

### *Test matrix*

The test matrix of the interaction tests is given in Table 4.

Table 4. Level ice interaction tests

Test #	Parameter	Ice drift length [m]	Carriage velocity [m/s]
<b>Test series 1000 to 4000 (X = 1, 2, 3, or 4)</b>			
X110	Joint, 15° heading	15 - 17	0.045 in sheet 1, 3, 4 0.2 in sheet 2
X120	Joint, 30° heading	14	
X130	Joint, 45° heading	10	
X140	Joint, 0° heading	10 - 12	
<b>Test series 5000</b>			
5110	Separated, 0° heading	15	0.045
5120	Separated, 0° heading, high speed	15	0.2
5130	Joint, 0° heading	10	0.045
5140	Joint, 45° heading	11	0.045

## **RESULTS**

### *Force-time measurements*

An example of the time series recorded is given in Figure 2 for the test run 3110. The load on LC2 was low and did not vary between the different test runs. It is therefore not presented further in the paper. The average load measured during the open water tests was subtracted from the reported loads. As Figure 2 shows the load initially increased before reaching a

plateau, or steady-state level both for the upper panel (LC1) and for the lowermost panel (LC3). Steady-state was defined visually, and the total horizontal force and the time to reach it ( $\Delta t$ ) were defined for each test. Steady-state was reached in all tests except for the rubble load (LC3) in test run 5130.

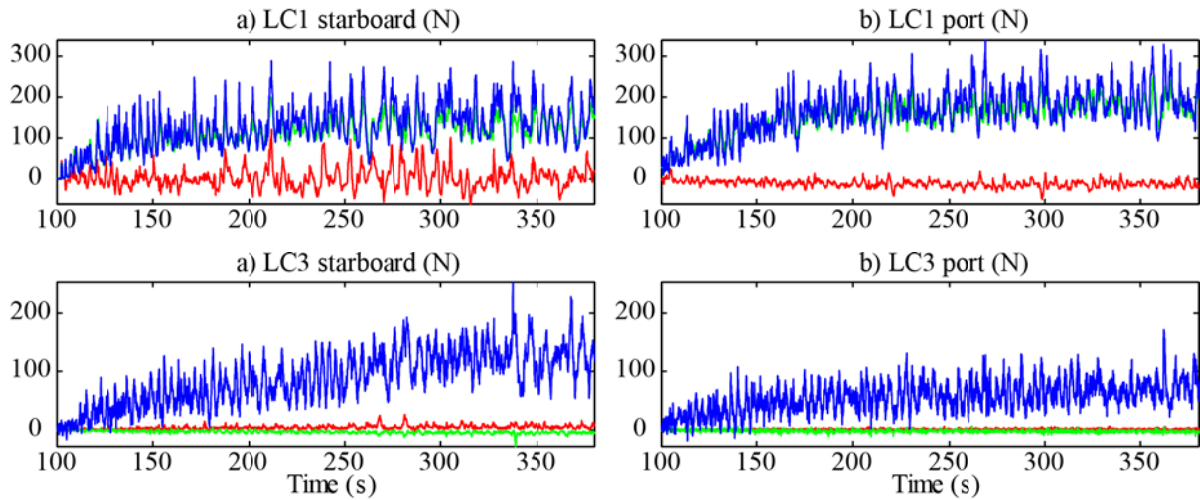


Figure 2. Load time series, run 3110, in a) starboard sub-structure, in b) portside sub-structure (blue line: horizontal normal load, red line: horizontal tangential load, green line, vertical load)

The time it took to reach steady state is plotted versus the ice incidence in Figure 3. Steady state was always reached earlier for LC1 than for LC3, but the difference decreased with increasing ice incidence.

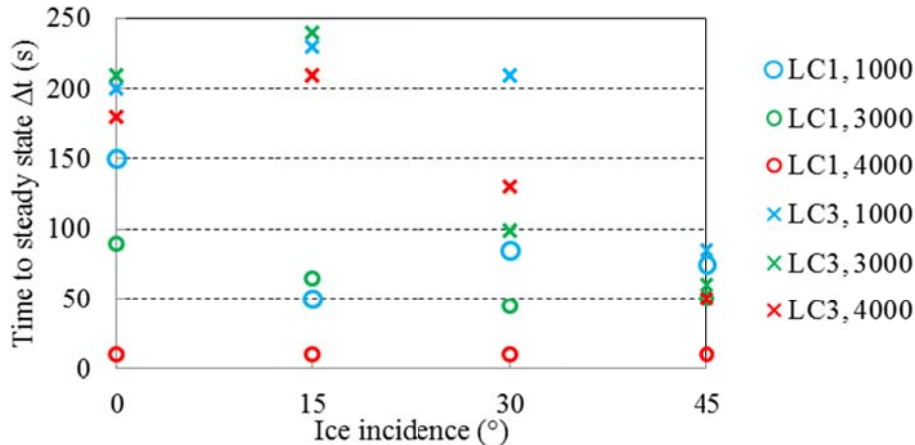


Figure 3. Average time to steady state as a function of ice incidence for the LC1 load (circles) and LC3 load (crosses).

#### ***Separated versus joint structure mode (variation of structure width)***

Figure 4 reports the average load at steady state for the joint and separated mode at  $0^\circ$  ice incidence (tests 5110 and 5130). The reported load is for the whole structure, i.e. for the sum of both sub-structures in the separated mode. The LC1 load level was the same for both configurations, while the LC3 load was two times as high in the joint mode. The load did not reach steady-state until the end of the test (300 s) in the joint mode, whereas in the separated mode it reached steady state after 155 s. The underwater videos showed that the rubble accumulated in a wedge form in front of the structure and as such it became larger in the joint mode.

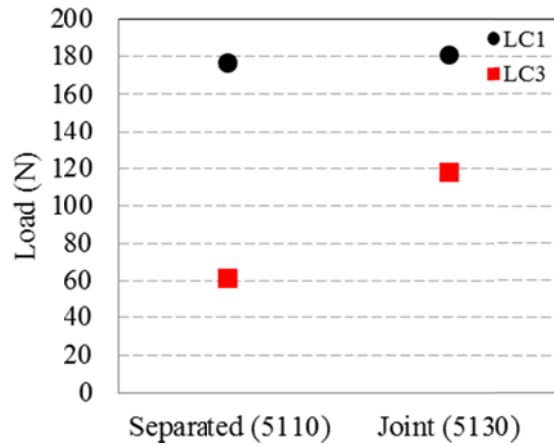


Figure 4. Sum of horizontal steady-state load on both sub-structures on the upper panel (LC1) and lowermost panel (LC3), in separated and joint mode (series 5110 and 5130).

### Ice parameter variation

Results from parameter variation of ice drift velocity, ice density, ice thickness and angle of incidence are given in Figure 5 a) for the load on panels LC1, and Figure 5 b) for the load on panel LC3. The figures show the average steady state load for all ice interaction tests with the structure in joint mode.

An increase in the ice thickness or the ice drift velocity clearly increased the load on the lower panel, whereas the decrease in ice density increased the loads on both panels (LC1 and LC3). All loads decreased for increasing angle of incidence. The ratio between the LC1 load in series 3000 (low density) and series 4000/5000 was more or less constantly two. Whereas for the LC3 panel the load in series 3000 and 4000 were similar for all angles, but the ratio between loads in 3000/4000 and the ones in 1000/5000 was constant and also about 2.

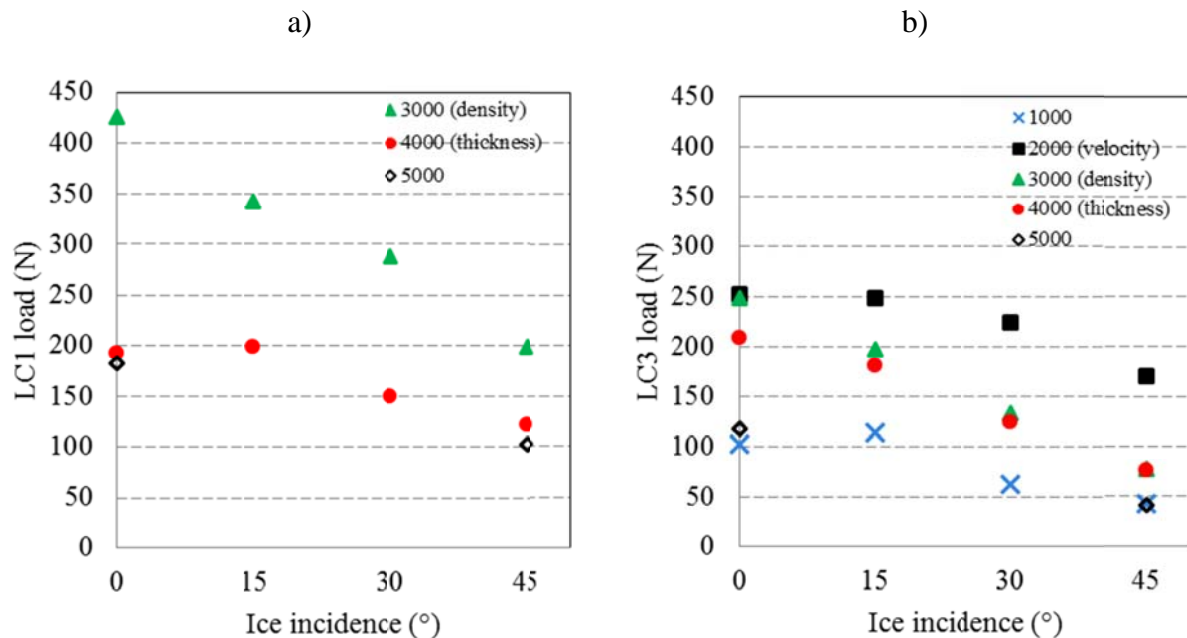


Figure 5. Average steady state load in function of ice parameters variation and ice incidence (joint structures), in a) panel LC1, in b) panel LC3.

## DISCUSSION

### *Nature of the load measured on LC1 and LC3*

The loads panels measured different components of the ice load:

- The upper LC1 panels extend 5 cm below the waterline and measured a waterline ice load. The intact ice interacted only with these panels, it was broken before the contact area slid down to the next load panel. The ice load measured on the LC1 panel include a load component to break the ice, but also load to push both the intact ice and underlying ice rubble down (including among others ventilation and inertia effects).
- The lower LC3 panels cover the vertical submerged part of the structures. Loads on these panels come from the action of the sub-surface rubble, but one cannot say that these panels monitor all loads from the sub-surface rubble.

The structure - intact ice - sub-surface ice interaction process is complex and the segmented panels cannot separate all the load contributions. However the upper LC1 panels monitor the load contribution at the waterline which is more affected by the ice breaking and sinking process, while the load monitored by the lower LC3 panels are more related to the sub-surface accumulation and clearing processes.

In the further discussion, the loads from LC1 will be referred as "waterline ice load", and loads from LC3 as "rubble loads".

### *Separated vs. joint structures (0° heading)*

The waterline load was not much affected by the structure configuration, separated or joined. The aspect ratio structure width over ice thickness is 66 and 33 respectively for the joined and separated configurations. This indicates that the structures are wide with regards to the ice breaking process, i.e. that 3D effects tend to have a limited effect.

The rubble load, on the other hand, was affected by the structure configuration. The total load doubled, it took more time to reach steady-state and more rubble accumulated in front of the structure in the joint mode than in the separated mode. It seems as if essentially the volume of accumulated rubble is a key parameter to determine the rubble load as long as the rubble is floating. In cases where the rubble grounds the friction between the grounded rubble and the seabed takes a portion of the total horizontal ice load (see e.g. the recent Palmer and Croasdale, 2013, p. 25).

### *Effect of ice properties*

The waterline action increased with increasing  $h_i$  and  $E$ . The ice breaking component is often considered to result from an elastic-plastic/brittle beam, or plate, on elastic foundation, and if so then increasing ice thickness and increasing stiffness will increase the load of the ice breaking component.

But in general the ice density was the ice property that had the most pronounced effect on the loads and the interaction process. Its effect on the waterline load was not because of the ice breaking component, but because of the two of the other components, the submerging of the broken piece and the submerging of the accumulated rubble. Both will increase with decreasing density. The buoyancy is a function of the difference between ice and water

density, the rubble porosity and its thickness. When the ice density was decreased by about 10% ( $100 \text{ kg/m}^3$ ) the buoyancy increased by 100%.

The direct effect of decreasing density is the increase of the buoyant load, so that any effort to push ice down becomes harder. This illustrates the coupled effect of the different components, and that the volume of accumulated rubble may be one (perhaps the) key point when estimating ice actions on sloping structures (which accumulate rubble).

The low density ice and the thicker and stiffer ice had almost identical effects on the rubble load relation to the heading. We think the effect is related to the buoyant load, caused by an increased volume of rubble in the case of stiffer and thicker ice, and caused by increased buoyancy forces in the case of low density ice. The rubble buoyant load can cause friction forces between the advancing level-ice sheet and the rubble which are transmitted to the structures. Therefore, an increased rubble buoyant force would cause an increased horizontal rubble load on the structure.

A possible effect of the flexural strength cannot be seen in our data. This does not mean that the flexural strength does not affect, but perhaps it is less important than the rubble accumulation. The formula for ice action on upward sloping structures given by ISO (2010) also predicts little effect of the flexural strength when ice rubble accumulates.

#### ***Effect of rubble ice on waterline load***

The fact that the waterline ice load steady state was always reached before the rubble ice load steady state (Figure 3) indicates that the accumulation of sub-surface rubble contributed to the increase of the waterline ice load (as predicted by the ISO 19906, 2010), but only up to a certain point. Above a certain volume of rubble, additional rubble had no effect on the waterline ice load. This observation explains why the waterline ice load was identical for the structure in joint and separated mode while the rubble volume and load were different. In both test configurations the accumulated amount of rubble was sufficient to cause the maximum waterline ice load.

## **CONCLUSION**

An experimental programme has been carried out in the HSVVA large ice basin where a wide sloping structure interacted with 5 different level ice sheets. The incoming ice velocity, the ice density, the ice thickness, the elastic modulus and the flexural strength were different for the different ice sheets. For each ice sheet four different ice incidence angles were tested ( $0^\circ$ ,  $15^\circ$ ,  $30^\circ$  and  $45^\circ$ ). And in series 5000 two different structure widths were tested. The main aim of the experiments was to investigate how the different parameters affected the ice load and the accumulation of rubble. Separate load panels measured the load in the water line and the load from the submerged rubble. The main conclusions are:

- A higher incidence increased the structure clearing capabilities and decreased the time to reach a steady state in the rubble accumulation.
- The waterline ice load steady state was always reached before the rubble load steady state, indicating that the accumulation of subsurface rubble contributes to an increase of the waterline ice load, but only up to a certain amount of rubble accumulation.
- The ice density was the most important ice property. A decreasing density increased all loads, but this effect decreased with increasing ice incidence. This is because a relatively mild decrease in density (10%) may cause an increasing the buoyant load of up to 100% and this caused the higher loads on the structure.

- A decrease in structure width (aspect ratio decreased from 66 to 33) doubled the rubble loads, but did not alter the water line load. The rubble load increase from about 1/3 and up to about 2/3 of the water line load.

## ACKNOWLEDGMENT

This project required the help of many participants who deserve the deepest acknowledgments: NTNU participants Henning Helgøy, Sergey Kulyakhtin, Wenjun Lu, and colleagues at Multiconsult Oda Skog Astrup, Juliane Borge, Hege Nilsen, and Arnor Jensen. Statoil financial contribution permitted to build the experimental set-up. The authors would also like to acknowledge the Norwegian Research Council through the project 200618/S60-PetroRisk and the SAMCoT CRI for financial support and all the SAMCoT partners.

The work described in this publication was supported by the European Community's 7th Framework Programme through the grant to the budget of the Integrated Infrastructure Initiative HYDRALAB-IV, Contract no. 261520. The authors would like to thank the Hamburg Ship Model Basin (HSVA), especially the ice tank crew, for the hospitality, technical and scientific support and the professional execution of the test programme in the Research Infrastructure ARCTECLAB.

## REFERENCES

- Croasdale, K.R., 1980. Ice forces on fixed, rigid structures. In: CRREL Special Report 80-26, Working Group on ice forces on structures. A State-of-the-Art Report. Int. Association for Hydraulic Research, Section on ice problems. U.S. Army CRREL, Hanover, NH, USA, pp. 34-103.
- Croasdale, K.R., Cammaert, A.B. and Metge, M., 1994. A Method for the Calculation of Sheet Ice Loads on Sloping Structures. Proc. 12th Int. Symposium on Ice, The Norwegian Institute of Technology, Trondheim, Norway, August 23-26, Vol. 2, pp. 874-875.
- Evers, K-U and Jochman, P., 1993. An advanced technique to improve the mechanical properties of model ice developed at the HSVA ice tank. Proceedings of the 12nd International Conference on Port and Ocean Engineering under Arctic Conditions, Hamburg, Germany, pp. 877-888.
- Frederking, R.M.W. and Timco, G.W., 1985. Quantitative analysis of ice sheet failure against an inclined plane. Proceedings of the 4<sup>th</sup> International Offshore Mechanics and Arctic Engineering Symposium, ASME, Dallas, pp 160-169.
- ISO/FDIS 19906, 2010. Petroleum and natural gas industries – Arctic offshore structures, ISO TC 67/SC 7. Final Draft International Standard, International Standardization organization, Geneva, Switzerland, 434p.
- Kulyakhtin, S., Høyland, K., Astrup, O., Evers, K-U., 2013. Rubble Ice Transport on Arctic Offshore Structures (RITAS), part III: analysis of model scale rubble ice stability. Proceedings of the 22nd International Conference on Port and Ocean Engineering under Arctic Conditions, Espoo, Finland.
- Lu, W., Serré, N., Evers, K-U., 2013. Rubble Ice Transport on Arctic Offshore Structures (RITAS), part IV Tactile sensor measurement of the level ice load on inclined plate. Proceedings of the 22nd International Conference on Port and Ocean Engineering under Arctic Conditions, Espoo, Finland.

- Paavilainen, J., Tuhkuri, J. and Polojärvi, A., 2011. 2D numerical simulations of ice rubble formation process against an inclined structure. *Cold Regions Science and Technology*, 68(1–2): 20-34.
- Paavilainen, J. and Tuhkuri, J., 2013. Pressure distributions and force chains during simulated ice rubbing against sloped structures. *Cold Regions Science and Technology*, 85(0): 157-174.
- Palmer, A and Croasdale, K., 2013. *Arctic Offshore Engineering*, World Scientific, ISBN 978-981-4368-77-3, 357 p.
- Schwarz, J., Frederking, R., Gavrillo, V., Petrov, I.G., Hirayama, K., Mellor, M., Tryde, P. and Vaudrey, K.D., 1981. Standardized Testing Methods for Measuring Mechanical Properties of Ice; *Cold Regions Science and Technology*, Vol. 4, pp. 245-253.
- Serré, N., Liferov, P., 2010. Loads from ice ridge keels – experimental vs. numerical vs analytical. *Proceedings of the 20th IAHR International Symposium on Ice*, June 14 to 18, Lahti, Finland.
- Serré, N., Repetto, A., Høyland, K.V., 2011. Experiments on the relation between freeze-bond and ice rubble strength, part I: shear box experiments, *Proceedings of the 21st International Conference on Port and Ocean Engineering under Arctic Conditions*, July 10-14.
- Serré, N., Lu, W., Høyland, K., Bonnemaire, B., Borge, J. and Evers, K-U., 2013. Rubble Ice Transport on Arctic Offshore Structures (RITAS), part II: 2D model scale study of the level ice action. *Proceedings of the 22nd International Conference on Port and Ocean Engineering under Arctic Conditions*, Espoo, Finland.
- Timco, G., 1991. The vertical pressure distribution on structures subjected to rubble forming ice, *11th International Conference on Port and Ocean Engineering under Arctic Conditions*, St.John's, Canada, pp. 185-197.